Electronic supplementary Information

Multifunctional fluorescent SPIONs display exceptional optical/magnetic contrast and enhanced photoconductivity in interdigitated electrode based photoresponsive devices

Ashish Tiwari [a,b]* Ayan Debnath[c], Mohamad G. Moinuddin[d], Aamir Mushtaq[e], Anup Singh[c], Satinder K. Sharma[d], and Jaspreet K. Randhawa[a]*

[a]School of Mechanical and Materials Engineering, Indian Institute of Technology Mandi, Himachal Pradesh, India-175005

[b]Faculty of Biomedical Engineering, Technion-Israel Institute of Technology, Haifa, Israel-3200003

[c]Center for BioMedical Engineering, Indian Institute of Technology Delhi, New Delhi, India-110016

[d]School Computing and Electrical Engineering, Indian Institute of Technology Mandi, Himachal Pradesh, India-175005

[e]Department of Materials Science and Engineering, Ohio State University, Ohio 43210, United States

Corresponding Author Address

Dr. Jaspreet Kaur Randhawa

Associate Professor

School of Engineering, Indian Institute of Technology Mandi, India

Email: jaspreet@iitmandi.ac.in

Table of content

Experimental

Materials and methods

Dimethyl-amino-methyl ferrocene, hydrogen peroxide, acetone and phosphate buffer solution (PBS) were purchased from Sigma Aldrich. Solvents used in synthesis and other studies were of analytical chemical grade. All chemicals were used without further purification.

Single step hydrothermal synthesis

In a typical synthesis, dimethyl-amino-methyl ferrocene (0.20 g) was dissolved in acetone solution (60 mL). After intense sonication for 1 hour, 5 mL of hydrogen peroxide solution was slowly added in the above solution, which was then vigorously stirred for 30 minutes under magnetic stirring. The solution was transferred to a 100 mL Teflon-lined stainless-steel autoclave. After sealing, the autoclave was heated and maintained at 220°C for 48 hours. The autoclave was then cooled naturally to room temperature. The black supernatant was carefully separated using a magnet. The brown precipitate was then washed with acetone three times. Finally, the brown precipitate was dried in a vacuum oven to get nitrogen-doped carbon-coated ultrasmall superparamagnetic iron oxide core-shell nanoparticles (SPIONs). Further, the black supernatant was purified through column chromatography to obtain nitrogen-doped carbon dot nanoparticles (NCDs). The products were used for further characterization and studies.

Magnetic separation and purification methods

After the synthesis, a magnet was used to separate both the brown precipitate and black supernatant from the reaction mixture. The core-shell SPIONs were collected from brown precipitate, washed with acetone, and dried to get the purified sample. On the other hand, the black supernatant after the separation was subjected to column chromatography using the standard protocol. In this purification method, a silica gels column chromatography was performed in ethyl acetate and hexane solvent to get the purified NCDs sample. Further, the purified NCDs sample was analyzed by NMR spectra to confirm the pure phase of carbon dot. In the embodiment of this aspect, we establish a separation method and a

purification process subjecting for the ideal and pure products after a single step hydrothermal synthesis wherein the nitrogen doping was achieved in-situ during the synthesis under experimental conditions.

Material characterizations

X-ray diffraction (XRD) patterns were obtained using a Rigaku Smart Lab diffractometer. The measurements were conducted using CuKα radiation over the 2θ range of 5° to 80°, with a scanning rate of 2°/min. Particle size analysis and elemental mapping were performed using FEI Tecnai TEM (transmission electron microscopy) with STEM-HAADF (scanning transmission electron microscope high angle annular dark field) imaging. The TEM operated at an acceleration voltage of 200 kV. Surface morphology was carried out using FESEM (field emission scanning electron microscopy) on a NOVA NanoSEM 450 instrument. The FESEM was operated at an accelerating voltage of 10 kV. UV−vis spectroscopy measurements were performed using a Shimadzu U-2450 UV−vis spectrophotometer, covering the wavelength range of 800−200 nm. Fluorescence measurements were recorded using a Horiba spectrophotometer, operating within the range of 800 to 200 nm. FTIR spectroscopy analysis was conducted using an Agilent Technologies Cary 6000 series instrument, covering the wavelength range from 400 to 4000 cm^{-1}. Magnetic properties were analyzed using a SQUID vibrating sample magnetometer (VSM) under a vibrating magnetic field of 4T at 300 K. Raman measurements were carried out using a Horiba LABRAM high-resolution Raman spectrophotometer, utilizing a 534 nm He−Ne laser. Hydrodynamic size and zeta potential were studied using the dynamic light scattering (DLS) method. NMR measurements were performed on a Joel India-JNM ECX-500 instrument, with the deuterated solvent $CDCl_3$ used for the NMR scans of NCDs.

Phantom Preparation for MRI scanning

MR imaging was performed following the reported literature [1]. To facilitate MRI scanning, a base solution containing 1.5% agarose was prepared. This base solution was put into a large cylindrical beaker with a capacity of 2 liters, and nine smaller test tubes with a diameter of 15 mm. In each of the small test tubes, different concentrations of iron were added to create a range of concentrations. Specifically, the concentrations used were 0.01 mM, 0.03 mM, 0.05 mM, 0.10 mM, 0.20 mM, and 0.50 mM. These small test tubes, labelled as phantoms 1 to 6, were inserted vertically into the large

cylindrical beaker, with the small phantoms positioned in a circumscribed manner within the larger phantom. This setup allows for the evaluation of different iron concentrations during the MRI scanning process.

Magnetic resonance imaging (MRI) and relaxivity studies

MRI experiments were performed to generate T2 and T1 maps, which provide valuable information about tissue properties and contrast. MRI experiments were conducted using a 3T whole-body MRI system (Ingenia, Philips Healthcare, The Netherlands) equipped with a 16-channel receive-only coil. T2 mapping data was acquired utilizing the vendor-supplied T2 mapping pulse sequence, which allowed for the acquisition of multiple echoes. The MRI protocol included a field of view (FOV) of 200x200, matrix size of 256x256, a slice thickness of 6 mm, and a total of 12 slices. The repetition time (TR) was set to 6000 ms, and the echo times (TE) used were 30, 60, 90, 120, 150, 180, and 210 ms. In addition to T2 mapping, MRI data for T1 mapping was obtained using an inversion recovery-based pulse sequence. The inversion times (TI) used in this sequence were as follows: 100, 300, 500, 700, 1000, 1500, 2000, 2500, 3000, and 3500 ms. These specific TI values were selected to capture the desired range of T1 relaxation times.

Relaxivity mapping

MRI images were processed using in house written programs in MATLAB. Voxelwise T_2 map was generated by fitting signal intensity data corresponding to different TEs to following mono-exponentially decaying function:

$$S(TE) = A \times e^{-\frac{TE}{T_2}} \qquad [1]$$

ROIs were drawn over small phantoms and average T2 values were computed for each ROI. $R2 = 1/T_2$ values were computed. Transverse Relaxivity (r2) of contrast agent is estimated using following equation:

$$R_2 = R_{20} + r2 \times C \qquad [2]$$

Where R_2 is concentration dependent relaxation time and R_{20} is relaxation time of base solution or agarose without contrast agent.

Magnetic force microscopy (MFM) measurements

In the magnetic field microscopy experiments, the primary objective was to measure the magnetic moment of individual nanoparticles. To achieve this, the nanoparticles were first deposited onto a silicon wafer, providing a suitable substrate for the analysis. The magnetic field microscopy technique involves using a specialized microscopy setup capable of detecting and characterizing magnetic fields. This setup typically includes an atomic force microscopy (AFM) equipped with high-resolution type of scanning probe microscopy (Bruker, Dimension ICON PT). The imaging studies were conducted in tapping mode with a scanning rate of 0.9 Hz. The silicon wafer with the deposited nanoparticles was carefully positioned within the microscope setup, ensuring optimal alignment for accurate measurements. The height between tip and sample surface was 50 nm. We used 500 Gauss of magnetic field to magnetize the AFM tip. The magnetic field probe, which can sense and quantify magnetic fields, was then brought into proximity with the nanoparticles. As the magnetic field probe interacts with the nanoparticles, it detects and measures the magnetic fields generated by the individual particles. The magnetic moment of each nanoparticle, which is a measure of its inherent magnetism, can be derived from the detected magnetic field.

Z-scan measurements for non-linear optical behavior

In the Z-scan experiments, we first drop casted the core-shell SPIONs on a glass substrate using a spin coating method. The Z-scan measurements were performed at two laser powers using the 800 nm wavelength of femto-second pulsed laser. The PL emission spectra was recorded on a Femtosecond spectroscopy microscope using the parameters as described previously reported literature. [2]

Cell culture studies and in vitro cytotoxicity assays of core-shell SPIONs

The SH-SY5Y neuroblastoma and HT-29 human colorectal adenocarcinoma cells used in this study were obtained from the National Centre for Cell Science (NCCS) in Pune, India. Upon reaching the desired confluency, the cells were seeded in a 96-well plate at a density of 5000 cells per well and

allowed to adhere overnight. Subsequently, the cells were treated with varying concentrations (0-50 µg/mL) of core-shell SPIONs. After 24 and 48 hours of incubation, 20 µL of 3-(4, 5-dimethylthiazol-2-yl)-2,5-diphenyl tetrazolium bromide (MTT) was added and incubated for 3 hours. Following this, the cells were dissolved in 100 µL of dimethyl sulfoxide (DMSO), and the absorbance was measured at 570 nm using a Tecan Infinite M200 PRO plate reader, with 650 nm as a reference wavelength.

Confocal laser scanning microscopy studies of core-shell SPIONs

The cellular internalization experiments were conducted following a previously described method. To perform confocal studies, SH-SY5Y neuroblastoma and HT-29 human colorectal adenocarcinoma cells were seeded on a coverslip in a 6 well plate and allowed to attach for 24 hours. Subsequently, the cells were exposed to a concentration of 10 µg/ml of SPIONs for a duration of 3 hours. Imaging was performed using a Nikon Eclipse Ti-U inverted confocal microscope.

Fabrication of semiconductor device of core-shell SPIONs

A photo-sensor based on µ-IDE-Pt/SPIONs was fabricated using standard semiconductor processing techniques. Scheme S1 illustrates the step-by-step process of fabricating the µ-IDE (micro-interdigitated electrode) with a 50 µm half-pitch over a thermally oxidized silicon (100) substrate. Initially, the Si (100) wafer underwent RCA cleaning (Scheme S1a) followed by thermal oxidation to create a ~300 nm thick oxide layer (Scheme S1b) to minimize leakage current. The oxidized wafers were diced, and then a layer of S1813 photoresist (Thomas Kirchner Corp.) was spin-coated onto the wafer and baked at 110°C (Scheme S1c). Next, the pattern of the µ-IDE was defined using ultraviolet (~365 nm) exposure with the EVG-610 tool. The exposed photoresist was developed using MF-319 developer (Scheme S1d). Inert metals (Pt/Cr) were deposited onto the patterned wafer using a DC-Magnetron sputtering system with a base pressure of 10-6 mbar and a deposition rate of 2 Å/sec to achieve a smooth surface (Scheme S1e). The patterned µ-IDE was further processed by removing the unexposed photoresist using a standard photoresist stripper. The fabricated µ-IDE was then rinsed with IPA and dried using N_2 gas (Scheme S1f). Further, core-shell SPIONs were dissolved in methanol, which is non-reactive to -OH organic solvents. A 5-10 wt.% dispersion of core-shell SPIONs was

formed through stirring and ultrasonication for 40 minutes. TThen, the resulting uniform dispersion was spin-coated onto the Pt electrodes of the μ-IDE multiple times at 2000 rpm, with a small heating step at 70°C for 60 seconds after each spin coating cycle. After deposition, any excess sample coating was removed from the contact pad to facilitate electrical measurements. For I-V (current-voltage) characterization, a Keithley 4200 SCS tool was employed in a two-probe geometry. The I-V characteristics of the fabricated sensor were evaluated under two different illuminations: red light (1.15 mW/mm^2) and green light (1.88 mW/mm^2) using highly collimated lasers (Huonje laser).

Cell culture studies and in vitro cytotoxicity assays of NCDs

Cell culture studies and in vitro cytotoxicity assays were conducted against HeLa cells. Cell line was procured from the National Centre for Cell Science (NCCS) in Pune, India. Upon reaching the optimal confluency, the cells were seeded in a 96-well plate at a density of 5000 cells per well and allowed to adhere overnight. Subsequently, the cells were treated with varying concentrations (0-50 μg/mL) of NCDs. After 24 hours of incubation, 20 μL of 3-(4, 5-dimethylthiazol-2-yl)-2,5-diphenyl tetrazolium bromide (MTT) was added to each well and incubated for 3 hours. Subsequently, the cells were dissolved in 100 μL of dimethyl sulfoxide (DMSO), and the absorbance was measured at 570 nm with 650 nm as a reference using a Tecan Infinite M200 PRO plate reader. All the data are the mean±SD.

Confocal laser scanning microscopy studies of NCDs

In accordance with a previously established protocol, cellular internalization experiments were conducted. HeLa cells were seeded onto a coverslip in a 6 well plate and permitted to adhere for 24 hours. Following the attachment phase, the cells were treated with a concentration of 10 μg/mL of NCDs for a duration of 3 hours. Imaging was performed utilizing a Nikon Eclipse Ti-U inverted confocal microscope.

Reaction Chemistry

The optimization of reaction conditions involved adjusting parameters such as precursor concentration, reaction temperature, and the amount of oxidizing agent, resulting in the production of versatile core-shell nanoparticles. Analysis of the synthesis process revealed that variations in reaction parameters led to distinct nanostructures, featuring an iron oxide core and amorphous carbon shell structures. Notably, the morphology of the particles was greatly influenced by the reaction temperature and the amount of oxidizing agent employed during synthesis. Among the synthesized nanostructures, spherical particles exhibited superior contrast as core-shell structures in TEM and STEM images (**Figure 1**) and displayed monodispersity in terms of particle morphology. Moreover, the synthesis of core-shell SPIONs involved intricate chemical processes within the reaction medium. To provide a concise understanding of the mechanism, two proposed processes are outlined here. Initially, dimethyl-amino-methyl ferrocene and H_2O_2 were dissolved in acetone and heated to 220 °C in a sealed chamber, resulting in the decomposition of ferrocene into iron and cyclopentadiene. Subsequently, cyclopentadiene underwent decomposition, generating carbon/carbon-nitrogen species/radicals. These radicals, possessing high surface energy, agglomerated and formed larger carbon radicals under the high temperature conditions within the sealed chamber. Meanwhile, H_2O_2 decomposed, producing O_2, which oxidized the iron atoms to form iron oxide nanoclusters. During the oxidation process, Fe cations were generated, catalyzing the decomposition of H_2O_2 and yielding new free hydroxyl and carboxyl radicals. These free radicals accelerated the oxidation of iron, resulting in the formation of iron oxide nanoclusters, while simultaneously reacting with the free carbon radicals to render them hydrophilic through the formation of hydroxyl and carboxyl groups. These reactions occurred under high temperature and pressure conditions in the gaseous state. As the reaction progressed to supersaturation, the iron oxide nanoclusters agglomerated, forming the core structure, followed by the deposition of carbon/carbon-nitrogen species, hydroxyl groups, and carboxyl groups as a shell on the surface of the iron oxide core. The surface-adsorbed carbon radical species facilitated the uniform carbon coating on the iron oxide core. The presence of chemical bonding between the iron oxide nanocrystals and the surface-adsorbed groups was successfully confirmed through XPS and FTIR spectra.

Figures and Tables:

In this work, we have reported that carbon coating and nitrogen doping were achieved simultaneously during the synthesis. In brief, dimethyl-amino-methyl ferrocene was used as a precursor dissolved in acetone while hydrogen peroxide as an oxidizing agent. The mixture was put in a hydrothermal and kept in a heating oven. The reaction parameters such as precursor concentration, amount of hydrogen peroxide, reaction time and temperature were optimized as detailed in Table S1.

Table S1: Comparison of synthesis parameters for core-shell SPIONs.

Synthesis	Precursor (Dimethyl-amino-methyl ferrocene) (gm)	Hydrogen peroxide (ml)	Amount of solvent (ml)	Reaction time (hours)	Reaction temperature (°C)
Synthesis 1	0.05	5	60	48	220
Synthesis 2	0.10	5	60	48	220
Synthesis 3	0.15	5	60	48	220
Synthesis 4	0.20	5	60	48	220
Synthesis 5	0.25	5	60	48	220
Synthesis 6	0.30	5	60	48	220
Synthesis 7	0.35	5	60	48	220

The FESEM images and elemental analysis of solely prepared samples showed that when we used ferrocene, there was no nitrogen doping observed. However, we observed a uniform structure of core-shell SPIONs.

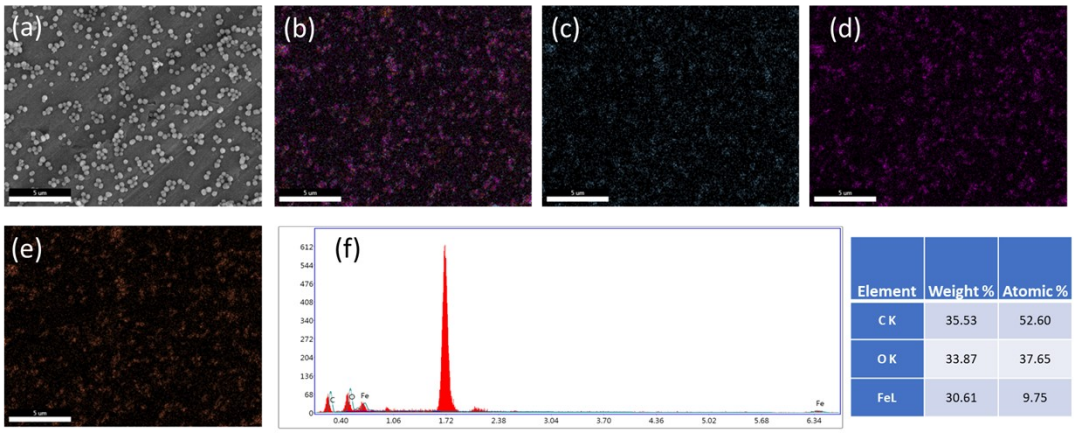

Figure S1. FESEM analysis of solely prepared core-shell SPIONs. (a) FESEM image, (b) overlay image, (c) carbon, (d) oxygen, (e) iron and (f) elemental analysis with table of percentage ratio respectively.

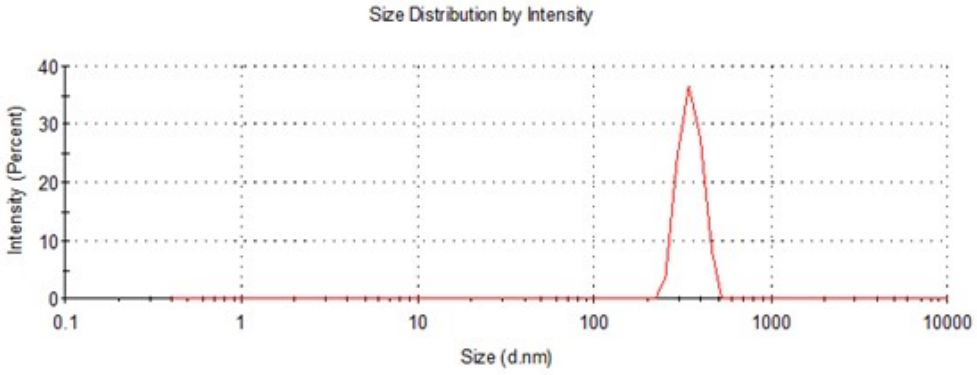

Figure S2. DLS analysis of core-shell SPIONs.

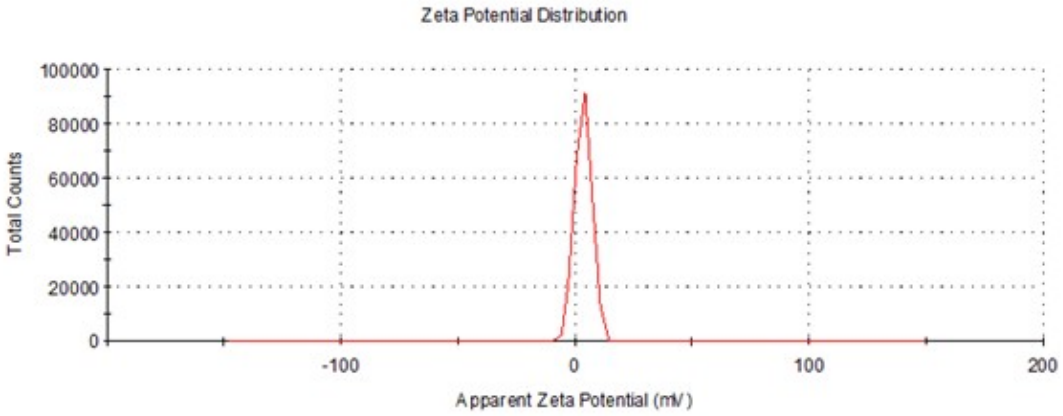

Figure S3. Zeta potential analysis of core-shell SPIONs.

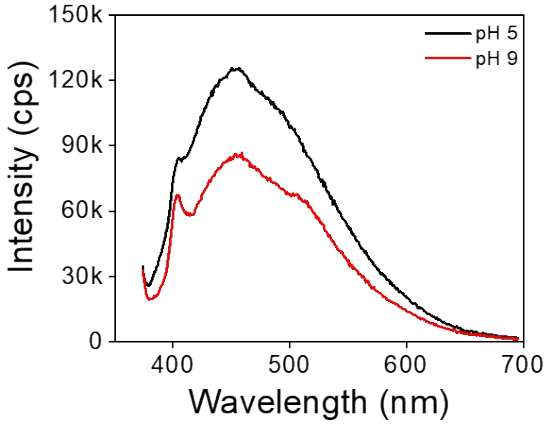

Figure S4. Emission spectra of core-shell SPIONs at two different pH mediums in PBS.

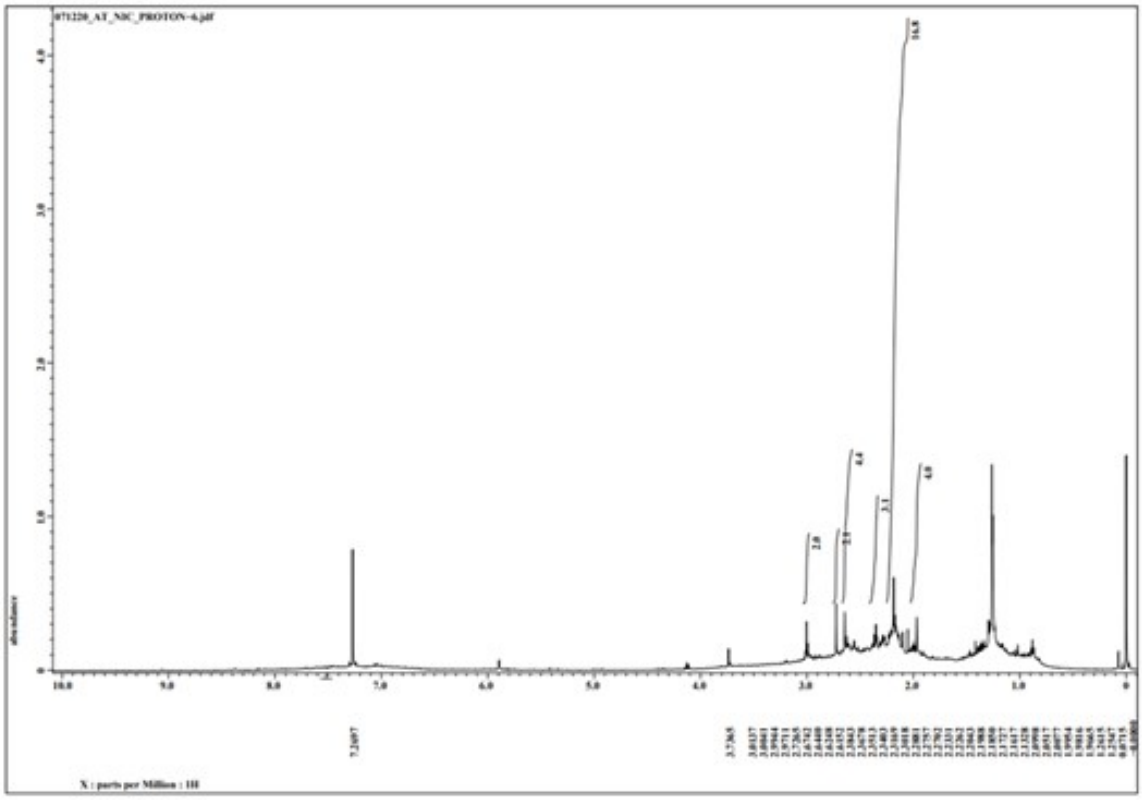

Figure S5. ^{1}HNMR spectra of NCDs.

Table S2. Comparison of relaxometry properties of clinical agents and core-shell SPIONs in the present work.

Contrast Agent	**R_2 ($mM^{-1}S^{-1}$)**	**Coating material**	**Comment**
DHAA-Fe_3O_4	121	DHAA	T1 and T2 agent
Ferumoxytol (Combidex)	89	Carboxymethyl-dextran	Clinical T1 and T2 agent,
Sinerem	65	Dextran	Clinical T1 and T2 agent,
ZES-SPIONs	10.5	Zwitterion-coated	T1 agent
Core-shell SPIONs (In this work)	156	Carbon	T2 agent

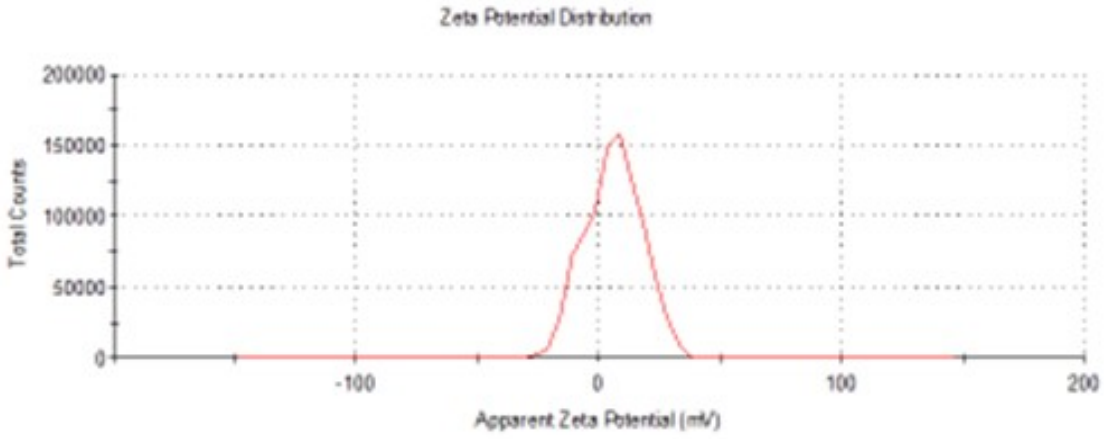

Figure S6. Zeta potential analysis of NCDs.

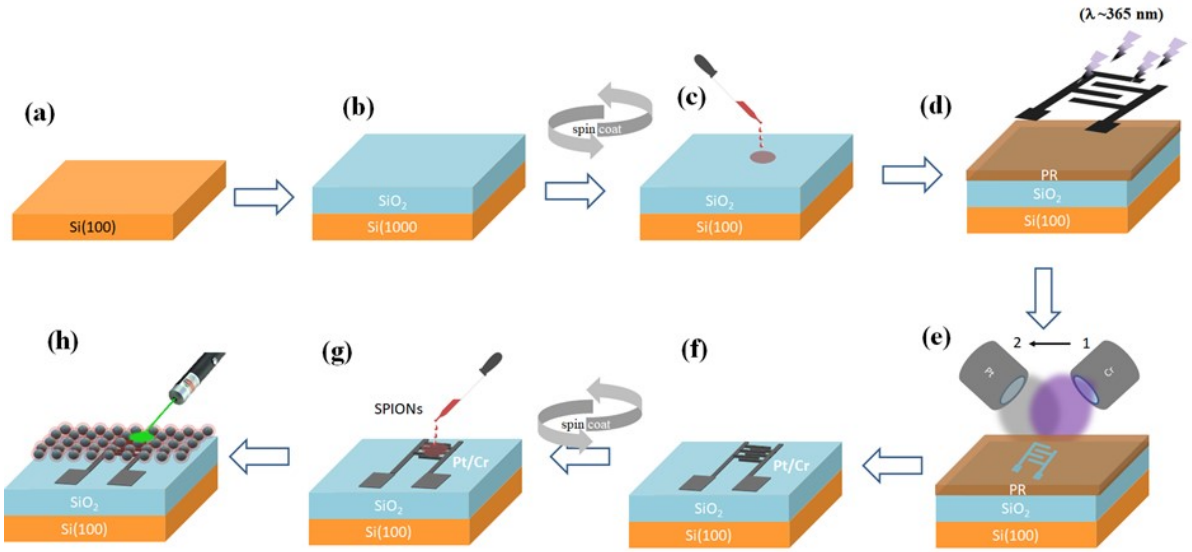

Scheme S1. Schematic process of the fabrication of noble metal-based μ-IDEs device. (a) deicing and cleaning of the wafer, (b) oxidation of Si (100) for smooth buffer layer ~ 300 nm, (c) spin-coating of S-1813 PR with the thickness of ~1 μm followed by PAB at 110 ^{o}C, (d) patterning of PR using NUV photo exposure with l-365 nm, (e) deposition of Pt/Cr over the patterned area. (f) lift-off process of PR and interdigitated electrode formation, (g) spin-coating of core-shell SPIONs, and (h) Electrical characterization with monochromatic light illumination.

References

1. Sengupta, Anirban, et al. "On differentiation between vasogenic edema and non-enhancing tumor in high-grade glioma patients using a support vector machine classifier based upon pre and post-surgery MRI images." European journal of radiology 106 (2018): 199-208.

2. Mushtaq, Aamir, et al. "Femtosecond induced third-order optical nonlinearity in quasi 2D Ruddlesden–Popper perovskite film deciphered using Z-scan." Materials Advances 3.22 (2022): 8211-8219.